



Article

CC(T) Specimen Load-Bearing Capacity Related to Yield Strength and Upper-Shelf Charpy-V Energy

Kim Wallin

K_W-solutions, Ltd., Heinäkuja 4A, 02760 Espoo, Finland; Kim.Wallin@kwsolutions.fi

Abstract: The load-bearing capacity of a CC(T) specimen (Center-Cracked Tension) in the ductile fracture regime is usually controlled by plastic collapse. If the material's tearing resistance is sufficiently low, the load-bearing capacity can drop below the plastic collapse value. Here, a recently developed simple fracture mechanics-based Charpy-V impact energy criterion for plastic collapse was used to provide a best estimate assessment of the CC(T) specimen load-bearing capacity.

Keywords: structural assessment; fracture mechanics; impact fracture; limit load; CC(T) specimen



Citation: Wallin, K. CC(T) Specimen Load-Bearing Capacity Related to Yield Strength and Upper-Shelf Charpy-V Energy. *Appl. Mech.* **2021**, *2*, 666–680. <https://doi.org/10.3390/applmech2040038>

Received: 14 July 2021

Accepted: 26 September 2021

Published: 28 September 2021

Publisher's Note: MDPI stays neutral with regard to jurisdictional claims in published maps and institutional affiliations.



Copyright: © 2021 by the author. Licensee MDPI, Basel, Switzerland. This article is an open access article distributed under the terms and conditions of the Creative Commons Attribution (CC BY) license (<https://creativecommons.org/licenses/by/4.0/>).

1. Introduction

Fracture mechanics is usually used mainly to ensure that a structure will not fail due to possible flaws. Normal engineering methods such as the one in Eurocode 3 focus mainly on avoidance of brittle fracture. If brittle fracture can be ruled out, it is commonly assumed that the structure will fail by plastic collapse and a limit load dimensioning is considered sufficient. However, if the material's ductile tearing resistance is sufficiently low, it is possible that ductile crack growth lowers the maximum load-bearing capacity below the plastic limit load. To safeguard against such events, a criterion for the ductile tearing resistance is also needed.

In a recent publication, a simple criterion for plastic collapse was developed based on the K_r/L_r ratio [1]. It postulates that if the K_r/L_r ratio is less than 0.4, the failure will be controlled by plastic collapse. K_r represents the ratio between the elastic crack driving force and the material's fracture toughness, corresponding to a specific fracture definition [1]. L_r represents the ratio between primary load and plastic limit load corresponding to yield strength [1]. The function relating K_r to L_r represents the reciprocal of a plasticity correction on the elastic crack driving force. The criterion results in a simple Charpy-V requirement to ensure that the maximum load will be controlled by the limit load.

The Charpy-V impact energy requirement is conservative as it is based on a conservative estimate of the crack driving force and it is based on a lower bound-type correlation between J_{1mm} (J-integral value corresponding to 1 mm crack extension) and K_{Vus} (Charpy-V impact energy at upper shelf), and the correlations have been developed for highly constrained bend specimens (SE(B) (single-edged bend) and C(T) (compact tension)). The requirement is not intended to provide a best estimate of the Charpy-V impact energy required to ensure plastic collapse. It is a general screening criterion for plastic collapse. When the requirement is fulfilled, the likelihood of reaching the plastic limit load is high. In the original publication [1], there was a lack of experimental validation of the developed requirement. The goal of this work was to validate the requirement using actual test data. The CC(T) specimen geometry was chosen because it mimics structures with mainly tension loading as is the basic assumption in Eurocode 3 (EN 1993-1-10).

Here, the method was used to assess the maximum load values of CC(T) specimens. When the method is used to make a best estimate assessment of lowly constrained CC(T) specimens, many of the aspects of the requirement need to be considered and modified.

1.1. The Basis of the Criteria

The $K_r/L_r = 0.4$ criterion allows the definition of a simple fracture toughness criterion for plastic collapse. The stress intensity factor in terms of load P can be expressed in the form of Equation (1) and the plastic limit load can be expressed in the form of Equation (2) [1],

$$K_I = \frac{P}{B \cdot W^{1/2}} \cdot f(a/W) \quad (1)$$

$$P_L = \sigma_Y \cdot B \cdot W \cdot F(a/W) \quad (2)$$

where K_I is the stress intensity factor, P_L is the limit load, P is the load, B is the specimen thickness, W is the specimen height, and σ_Y is the yield stress.

The functions $f(a/W)$ and $F(a/W)$ are application-specific geometry functions that can be found from various handbooks [2,3].

The ratio K_r/L_r corresponding to the limit load ($L_r = 1$) can then be written in the form of Equation (3) by inserting P_L from Equation (2) into Equation (1) [1]. The fracture toughness K_{IC} represents the true material's fracture toughness, not the linear-elastic fracture toughness. This means that K_{IC} can correspond to J-integral-based K_{JC} or to a point on the tearing resistance curve, expressed in the same units as the stress intensity factor, K . Equation (3) can be used for any geometry.

$$\frac{K_{r(L_r=1)}}{L_r} = \frac{\sigma_Y \cdot W^{1/2} \cdot f(a/W) \cdot F(a/W)}{K_{IC}} \quad (3)$$

Applying simplified equations for the stress intensity factor and the limit load and replacing the yield strength with the material's flow strength (σ_f), an upper bound estimate of the required fracture toughness to achieve plastic collapse is given by Equation (4) [1]. It is based on the maximum of Equation (3) for several different crack and loading geometries and contains a plasticity correction equal to 2.5, which corresponds to the typical level of plasticity at $L_r = 1$ [1].

$$\frac{K_{IC}}{\sigma_f \cdot \sqrt{W}} \geq 2 \Rightarrow \text{plastic collapse} \quad (4)$$

Equation (4) gives a conservative estimate of the crack driving force close to the plastic limit load. This needs to be matched with the material's tearing resistance. The publication [1] favored the use of the tearing resistance corresponding to 1 mm ductile crack growth (J_{1mm}). The use of an initiation definition, such as J_{IC} , is considered overly conservative.

The value of J_{1mm} was estimated from a well validated $J_{1mm} - KV_{us}$ correlation [1,4]. The previous work [1] made use of the 5% lower bound correlation in the form of Equation (5). The J-integral values need to be written in the form of K_{IC} , Equation (6), where E is the modulus of elasticity and ν is Poisson's ratio.

$$J_{1mm-5\%} = 193 \cdot \left(\frac{KV_{us}}{100} \right)^{1.28} \quad (5)$$

$$K_{IC} = \sqrt{\frac{J \cdot E}{(1 - \nu)^2}} \quad (6)$$

The publication [1] ended up with a simple Charpy-V impact energy requirement in the form of Equation (7).

$$KV(J_{1mm}) \geq \exp \left\{ 0.59 + 0.78 \cdot \ln(W) + \sqrt{\frac{\sigma_Y}{343}} \right\} \quad (7)$$

1.2. Modifications Specific to CC(T) Specimen

The CC(T) specimen has a very simple geometry (Figure 1). There are several stress intensity factor solutions for the CC(T) specimen [2]. Equation (8) is supposed to have

an accuracy of 0.1% for any proportional crack length a/W [2]. The corresponding limit load equation is very simple, due to the extremely low constraint of the specimen. It can simply be expressed in terms of a constant net section stress, Equation (9) [3]. The crack driving force equation corresponding to limit load thus becomes Equation (10). It includes the plasticity correction of approximately 2.5, as used in the original simplified method described above. Equation (10) is shown graphically in Figure 2. As seen from the figure, the maximum crack driving force is close to 2, as assumed in Equation (4).

$$K_I = \sigma \cdot \sqrt{\pi \cdot a} \cdot \left(1 - 0.025 \cdot \left(\frac{a}{W} \right)^2 + 0.06 \cdot \left(\frac{a}{W} \right)^4 \cdot \sqrt{\sec\left(\frac{\pi}{2} \cdot \frac{a}{W}\right)} \right) \quad (8)$$

$$\sigma_L = \sigma_f \cdot \left(1 - \frac{a}{W} \right) \quad (9)$$

$$\frac{K_{I(L_r=1)}}{\sigma_f \cdot \sqrt{W}} = \sqrt{\pi \cdot \frac{a}{W}} \cdot \left(1 - 0.025 \cdot \left(\frac{a}{W} \right)^2 + 0.06 \cdot \left(\frac{a}{W} \right)^4 \cdot \sqrt{\sec\left(\frac{\pi}{2} \cdot \frac{a}{W}\right)} \right) \cdot \left(1 - \frac{a}{W} \right) \cdot 2.5 \quad (10)$$

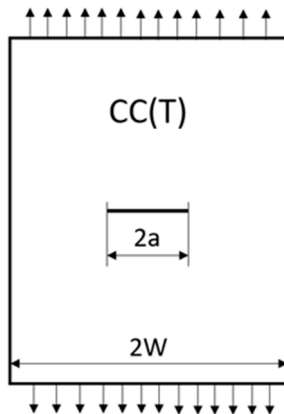


Figure 1. Definition of CC(T) specimen dimensions. The dimensions $2a$ and $2W$ are the crack length and specimen width, respectively.

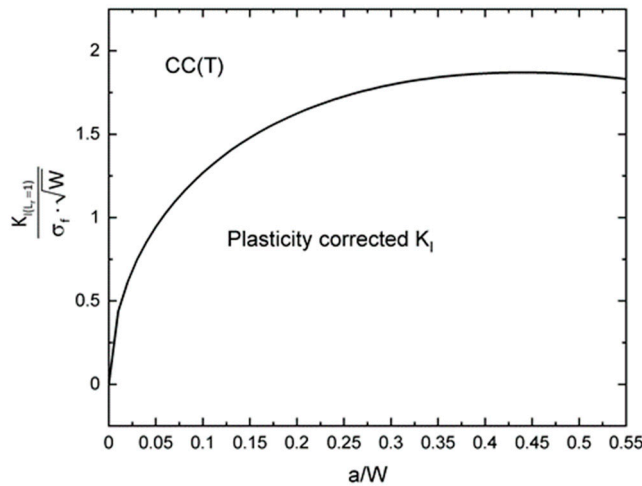


Figure 2. Plasticity-corrected crack driving force at limit load $\frac{K_{I(L_r=1)}}{\sigma_f \cdot \sqrt{W}}$ for a CC(T) specimen, as a function of relative crack length a/W .

The J_{1mm} –CVN_{us} correlation that is based on the 5% lower bound is not applicable for a best estimate. Instead, the median correlation should be used. This has the form of Equation (11) [1,4].

$$J_{1mm} = 269 \cdot \left(\frac{KV_{US}}{100} \right)^{1.28} \quad (11)$$

The above-described energy requirement does not account for constraint differences. Deeply cracked bend specimens experience a high stress triaxiality or constraint, because the yielding is contained due to the compressive stresses opposite of the crack. Single-cracked-tension-loaded specimens experience an uncontained yielding because the whole ligament is in tension and, thus, the stress triaxiality or constraint is much lower. The CC(T) specimen thus has a much lower constraint than the bend specimens used for the Charpy-V correlation, and this has a pronounced effect on the tearing resistance curve.

The T-stress, which is an elastic parameter, corresponds to the higher-order nonsingular term in the series expansion of the stress field equation. Even though the T-stress describes the nonsingular stress component in the direction of the crack plane, it also gives an approximation of the opening stress in the loading direction.

Figure 3 shows the effect of constraint, expressed in the form of T-stress at limit load, on the J-integral for a specific crack growth compared to a high-constraint configuration [5]. Deeply cracked bend specimens have positive T-stresses, whereas the CC(T) specimens have strongly negative T-stresses, as seen from Figure 4 [5]. The T-stress effect on the tearing resistance can be approximated by Equation (12) [5]. The accuracy of the constraint effect description is of the order of $\pm 15\%$.

$$\frac{J}{J_{T>0}} \approx \left\{ \exp - \left(\frac{\text{T-stress} - 100 \text{ MPa}}{1500 \text{ MPa}} \right) \right\}^2 \dots \text{T-stress} \leq 100 \text{ MPa} \quad (12)$$

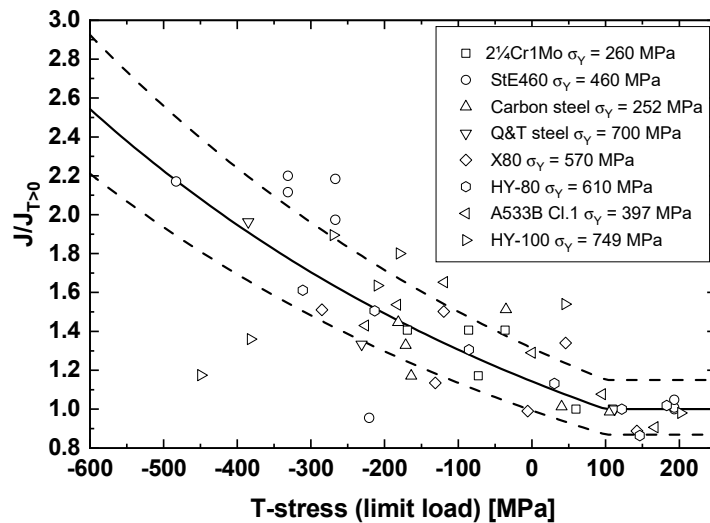


Figure 3. Effect of constraint expressed in the form of T-stress at limit load, on the J-integral for a specific crack growth compared to a high-constraint configuration ($J/J_{T>0}$) [5]. Dashed lines indicate $\pm 15\%$ uncertainty.

Figure 4 contains a fit to the individual T-stress data. It has the form of Equation (13) [5].

$$\frac{\text{T-stress}}{\sigma_Y} \approx -1.14 + 0.89 \cdot \frac{a}{W} + 0.152 \cdot \left(\frac{a}{W} \right)^2 - 0.495 \cdot \left(\frac{a}{W} \right)^3 \quad (13)$$

It is important to note that Equation (13) corresponds to limit load. If the net section stress (σ_{net}) is below the flow stress, Equation (13) needs to be multiplied by the ratio $\sigma_{\text{net}}/\sigma_f$.

The Q parameter is an elastic-plastic constraint parameter. A definition, in line with the T-stress, refers to the normalized distance between the actual tensile stress σ_{yy} at a

specified location in front of the crack and the matching value corresponding to the small-scale yielding solution for $T = 0$ [6]. It can be expressed in the form of Equation (14) [6].

$$Q \equiv \frac{\sigma_{yy} - (\sigma_{yy})_{T=0}}{\sigma_Y} \quad \text{at} \quad \theta = 0, \quad \frac{r \cdot \sigma_Y}{J} = 2 \quad (14)$$

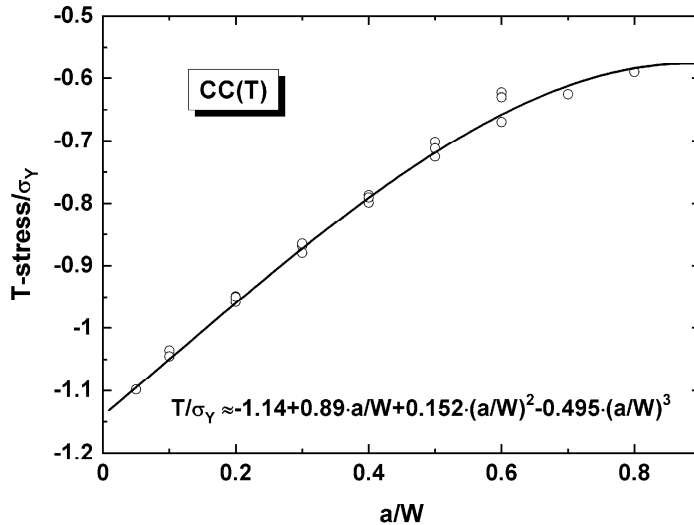


Figure 4. T-stress at limit load, normalized by yield strength, for a CC(T) specimen, as a function of relative crack length a/W [5].

Figure 5 shows a comparison of the yield stress-normalized elastic T-stress corresponding to limit load and the Q value corresponding to the load at J_{IC} , where the Q values have been collected from the references leading to Figure 3. Overall, the two parameters follow an approximate offset of 0.15. The T-stress underestimates very low Q values and overestimates very high values, but in the range $Q = -1$ to 0, the estimates generally differ less than 0.2, which is of the same order as the uncertainty in the parameter estimates. This provides validation for the use of Equation (12) to describe the constraint effect for ductile fracture.

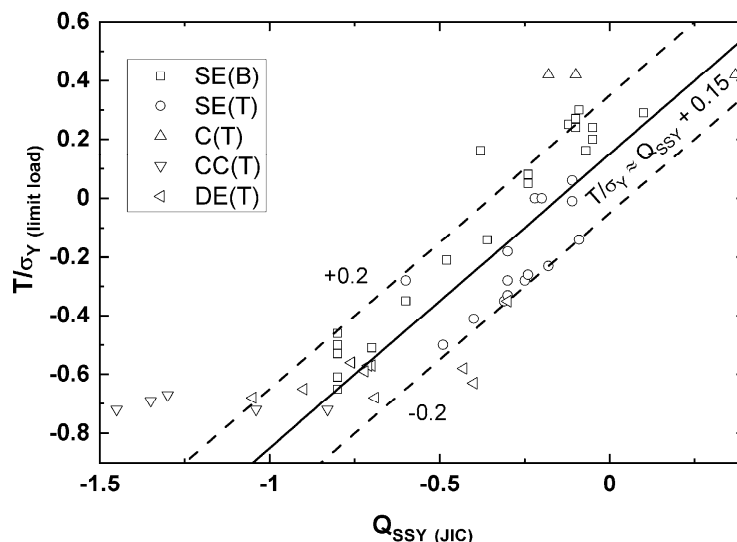


Figure 5. Relation between elastic T-stress at limit load (T/σ_Y) and elastic-plastic Q parameter at J_{IC} [5].

The constraint effect data in Figure 3 are verified only to a $J/J_{T>0}$ ratio of 2. Due to this, the constraint correction for the CC(T) specimens is limited to 2. This is in line with actual tearing resistance data for CC(T) specimens, as compared to C(T) specimen tearing resistance data shown in Figure 6 [7].

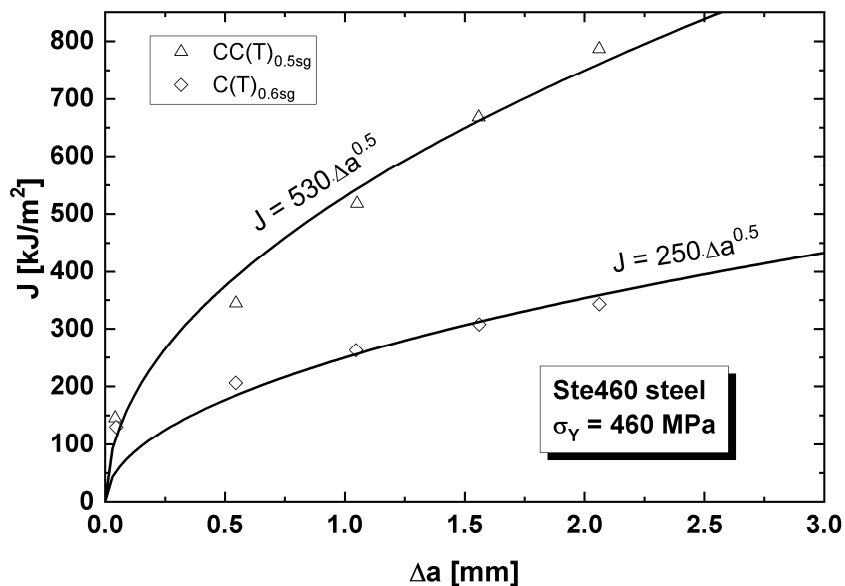


Figure 6. Comparison of CC(T) and C(T) specimen tearing resistance (J -integral versus crack extension Δa) for a medium-strength steel [7].

2. Materials and Methods

The data for the CC(T) tests were taken from [8–10]. Nine different steels with different mechanical properties were covered. Their mechanical properties are given in Table 1. The strength levels varied from moderate (325 MPa) to extra high (988 MPa). The Charpy-V upper-shelf energies, measured at ambient temperature, were in the range 85 J to 250 J. The specimens were CC(T) specimens with $W = 150$ mm and having varying crack lengths. The plate thickness varied between 20 and 40 mm, being in most cases 30 mm. The thickness dimension was not significant for the CC(T) specimens, when assessed in terms of nominal and net section stress. The first four steels had specimens with pre-fatigue cracks, whereas the other steels had specimens with narrow Electric Discharge Machining (EDM) notches. All tests were performed at room temperature. The specimens were loaded in tension under displacement control and, for this work, the maximum load during the test was used in the analysis. None of the specimens experienced unstable fracture prior to maximum load during the tests.

Table 1. Mechanical properties of the materials [8–10].

Material	σ_Y MPa	σ_U MPa	KV_{us} J	Ref.
S355N	364	526	250	[8]
S500M	584	639	227	[8]
S690QL	845	884	192	[8]
S960QL	988	1055	125	[8]
St52-3	403	594	200	[9]
St52-3	325	490	85	[9]
Steel A	420	640	200	[10]
Steel B	565	715	200	[10]
Steel C	755	835	120	[10]

The CC(T) test results for the three sets of steels are shown compiled in Figures 7–9, in the form of nominal stress at load maximum.

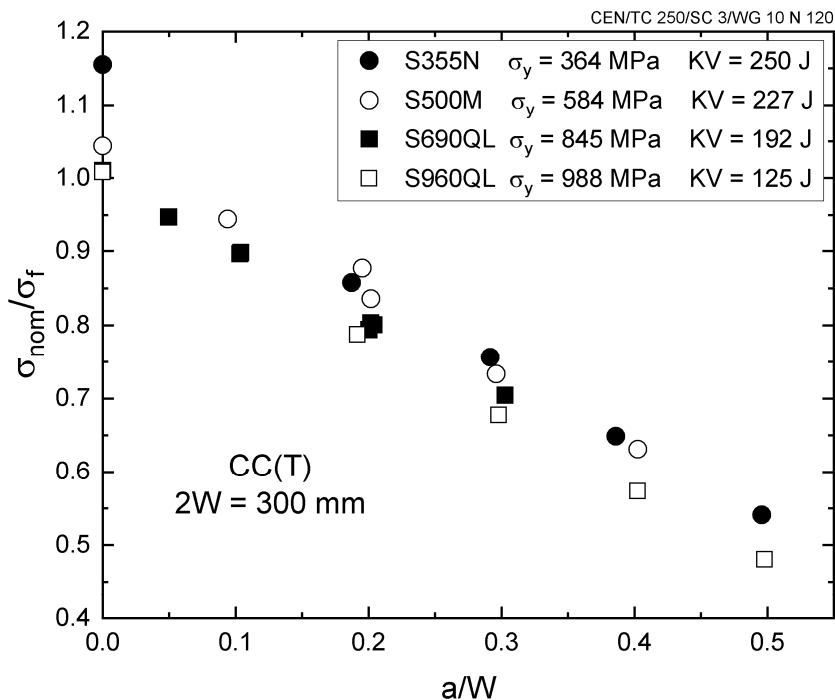


Figure 7. CC(T) test maximum load (nominal stress) values divided by flow stress for four different steels, as a function of relative crack length a/W [8].

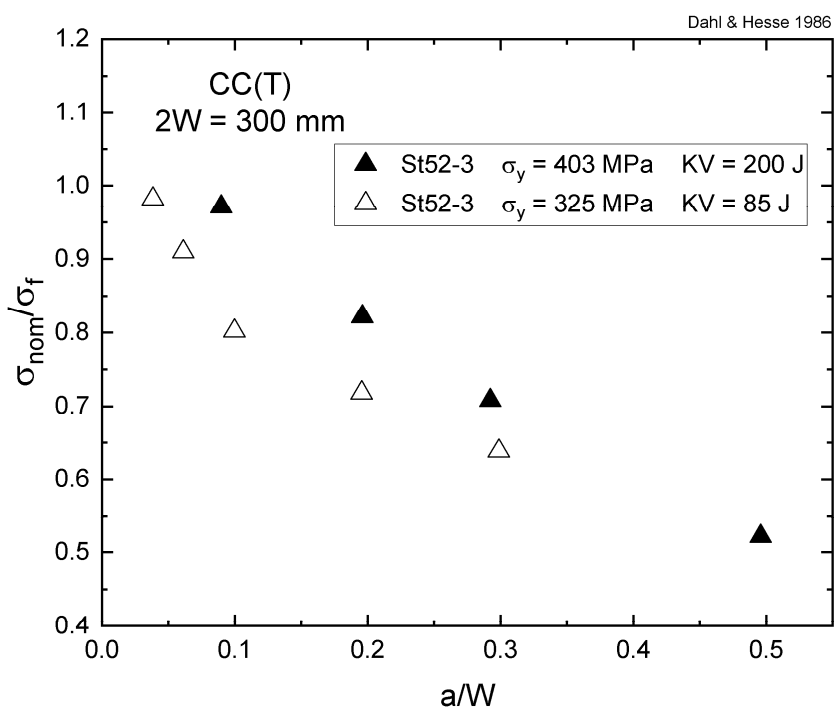


Figure 8. CC(T) test maximum load (nominal stress) values divided by flow stress for two different St52-3 steels, as a function of relative crack length a/W [9].

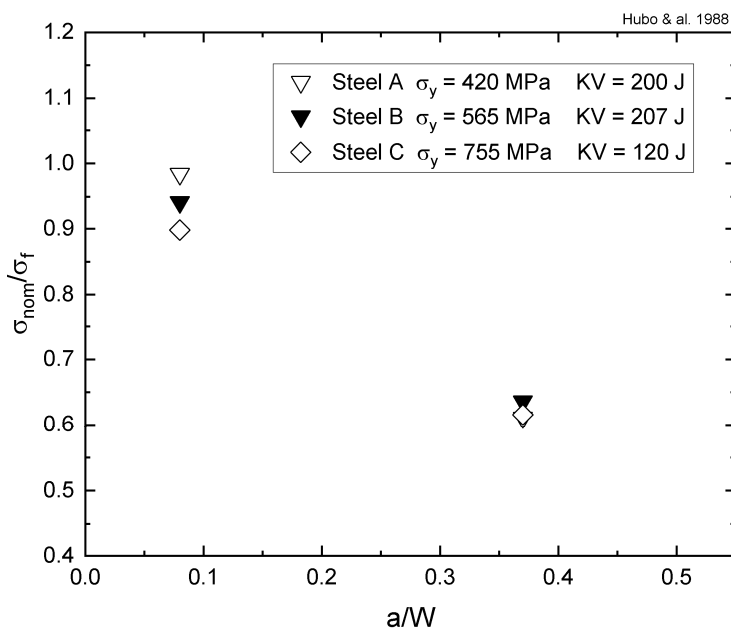


Figure 9. CC(T) test maximum load (nominal stress) values divided by flow stress for three different steels, as a function of relative crack length a/W [10].

3. Results

The individual test results were analyzed with Equations (10)–(13), to estimate the required Charpy-V impact energy to achieve the plastic limit load in terms of Equation (9). In cases when Equation (12) indicated a larger constraint effect on J than 2, the adjustment was limited to 2. This only occurred with the smallest crack length and higher-strength steels. Figures 10–12 show the measured proportional maximum net section stresses as a function of relative crack length. The results are comparable as all specimens had a width ($2W$) of 300 mm. The crack length does seem to have a pronounced effect on the maximum net section stress.

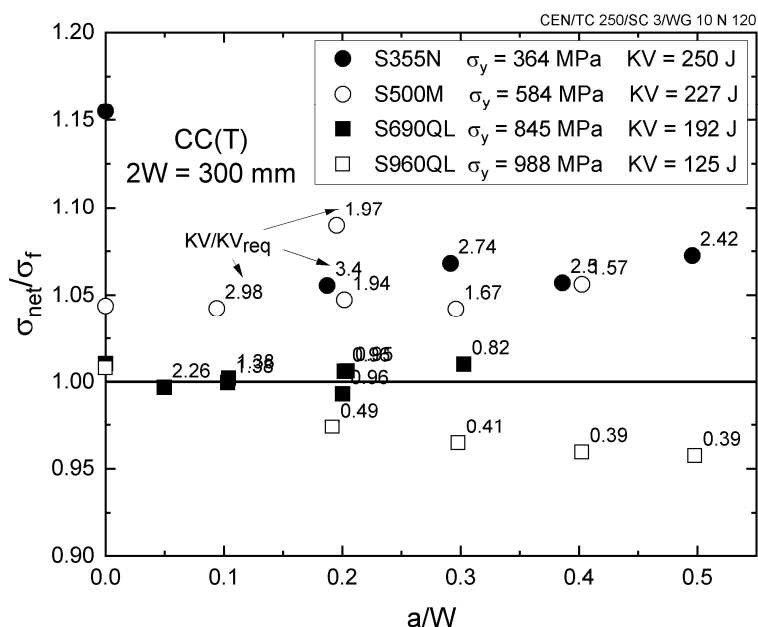


Figure 10. Net section stress values divided by flow stress for the data in Figure 7 as a function of relative crack length and related to the ratio between the Charpy-V impact energy and estimated required impact energy to obtain the plastic limit load.

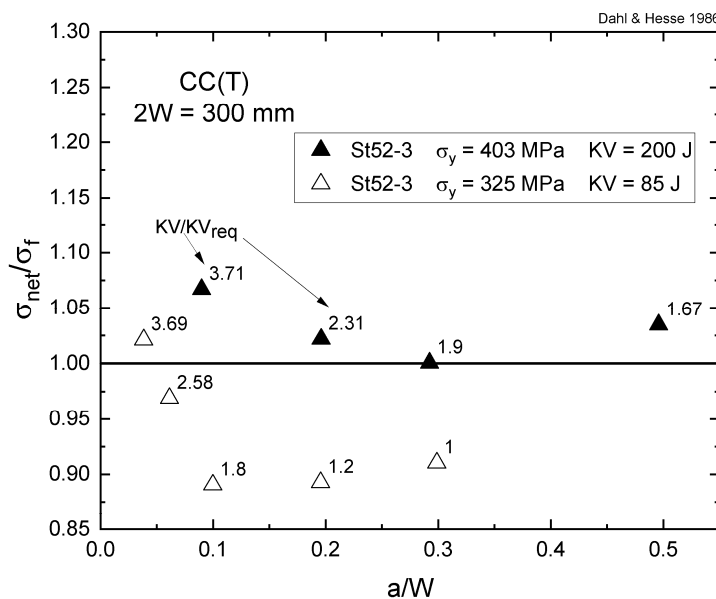


Figure 11. Proportional net section stress values divided by flow stress for the data in Figure 8 as a function of relative crack length and related to the ratio between the Charpy-V impact energy and estimated required impact energy to obtain the plastic limit load.

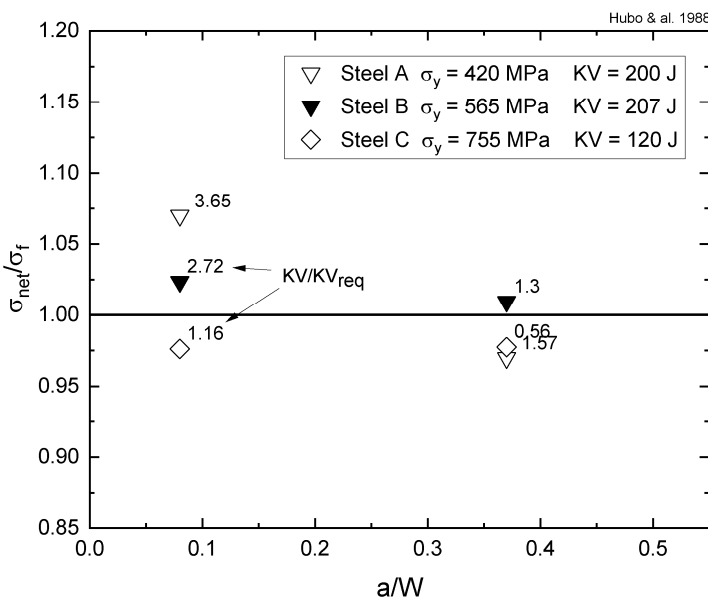


Figure 12. Proportional net section stress values divided by flow stress for the data in Figure 9 as a function of relative crack length and related to ratio between the Charpy-V impact energy and estimated required impact energy to obtain the plastic limit load.

The figures include the ratio between the Charpy-V impact energy and estimated required impact energy to obtain the plastic limit load. With some exceptions, there is a trend that a low maximum net section stress is related to a low ratio between the Charpy-V impact energy and estimated required impact energy.

This effect is examined more closely in Figure 13. With one exception, the results show a positive trend between proportional maximum net section stress and the ratio between real and required impact energy. The second St52-3 steel appears to differ from the general trend. Generally, considering that the estimates are average best estimates, the data tend to confirm that when the material's impact energy matches or is above the required value, the maximum net section stress equals or is above the plastic limit load.

value, based on flow stress. The variation in the results can be attributed to the scatter in the J-integral—Charpy-V correlation and to small ($\pm 5\%$) deviations in the flow strength.

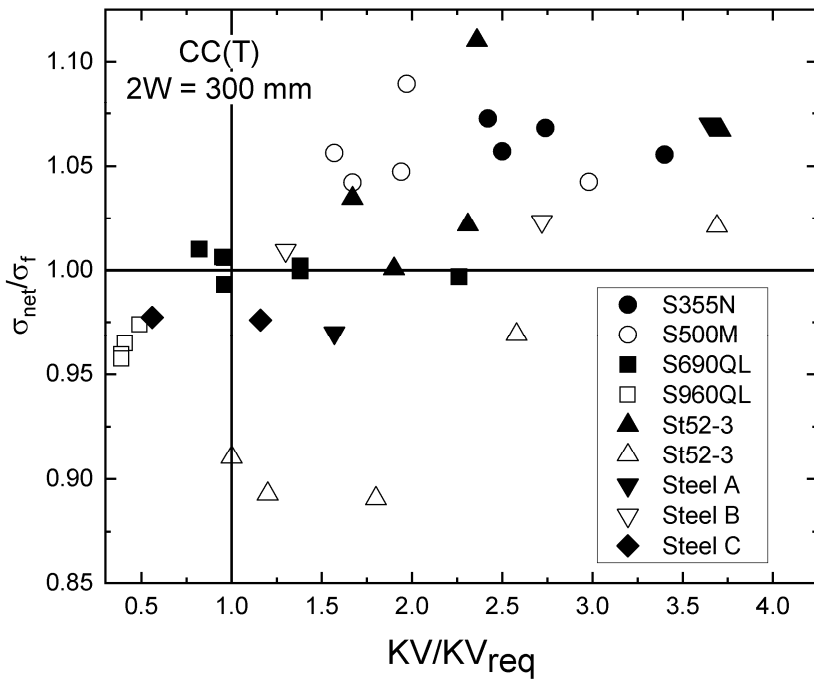


Figure 13. Compilation of proportional net section stress divided by flow stress as a function of ratio between the Charpy-V impact energy and estimated required impact energy to obtain the plastic limit load.

4. Discussion

The load-bearing capacity of CC(T) specimens is seen to be controlled by the material's flow stress, based on the net section stress in the ligament, provided the material's upper-shelf impact energy is sufficient. The second St52-3 steel seems to deviate from the general trend. For this steel, there are more test results from different-size CC(T) specimens [11]. The results refer to specimen widths in the range $2W = 120\text{--}600$ mm and a variety of relative crack lengths. The material and plate thickness (30 mm) are the same as for the second St52-3. Most 300 mm test results are the same as in Figure 8. The nominal stress at load maximum, as a function of relative crack length for the different specimen widths, is shown in Figure 14 [11]. The maximum nominal stress is clearly both dependent on the relative crack length and the specimen width.

The data in Figure 14 were analyzed similarly to the data for a constant specimen width. The result, in the form of the ratio between the Charpy-V impact energy and estimated required impact energy to obtain the plastic limit load, is shown in Figure 15. The results confirm that the crack driving force directly affects the maximum net section stress. It is unlikely that the Charpy-V energy would be much lower than 85 J. Even though the correlation between J-integral and Charpy-V energy is based on the median correlation, the trend with low net section stress values in Figure 15 cannot be explained by the uncertainty in the correlation alone, as seen from Figure 16. The calculation in this case is performed using the 5% lower-bound Charpy-V-J correlation, as given in Equation (5). The constraint correction is also conservatively taken as 1. Even for this conservative estimate, the net section stress values are low with respect to the expectations. One possible explanation is that the true flow stress of this St52-3 is 10–15% lower than assumed based on the reported tensile test results.

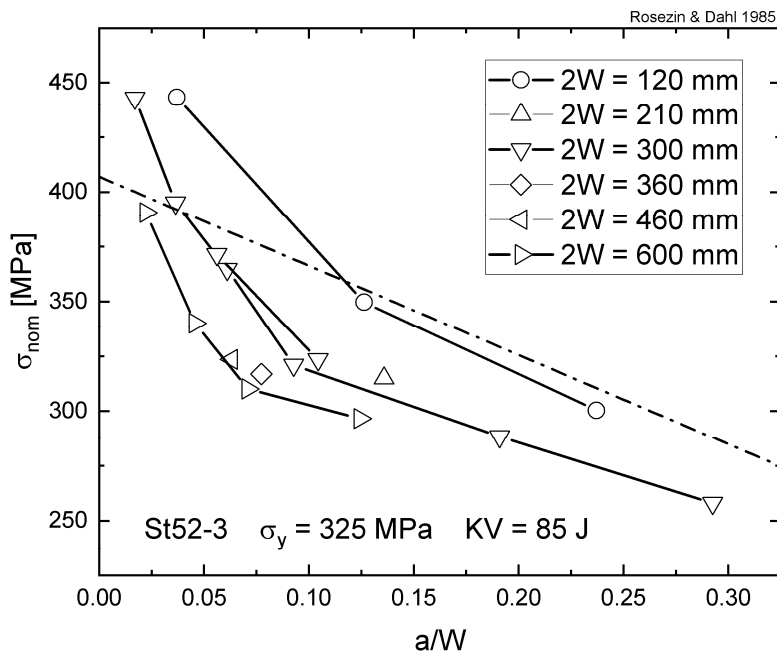


Figure 14. CC(T) test maximum load (nominal stress) values for different specimen widths, as a function of relative crack length a/W [11].

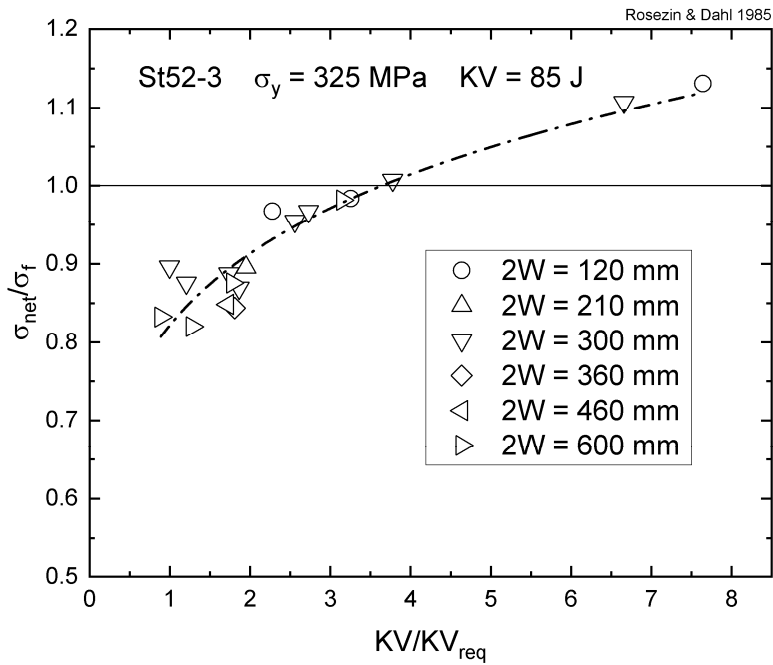


Figure 15. Compilation of proportional net section stress divided by flow stress as a function of ratio between the Charpy-V impact energy and estimated required impact energy to obtain the plastic limit load for the second St52-3 steel.

The assumption of a lower-than-assumed flow stress is strengthened by a second set of test results for the same St52-3 steel [11]. These test results correspond to a 15 mm plate thickness. The mechanical properties are higher than for the 30 mm plate, but the steel composition is identical. The material's impact energy is not known, but from experience, it is expected to be higher than for the 30 mm plate. The data are comprised of a set of different-width CC(T) specimens with a constant initial flaw with $2a = 15$ mm. The data, in the form of a maximum net section stress in relation to the flow stress, are reproduced in Figure 17, as a function of specimen width [11]. In addition, in this case, the maximum net

section stress is lower than expected, similar to the 30 mm-thick plate data. For comparison, a test result for a similar-strength Fe510 steel with identical flaw size ($2a = 15$ mm) and plate thickness (15 mm) [12] is included in Figure 17. The behavior of the Fe510 steel is similar to those of all the other steels in the study. This is an additional indication that the true flow stress of this St52-3 is 10–15% lower than assumed based on the reported tensile test results.

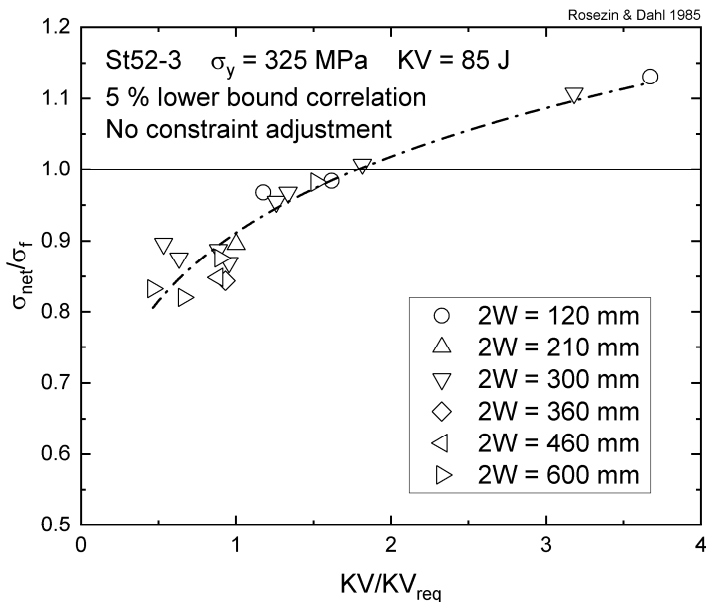


Figure 16. Compilation of proportional net section stress divided by flow stress as a function of ratio between the Charpy-V impact energy and estimated required impact energy to obtain the plastic limit load for the second St52-3 steel. Calculation based on conservative correlation, Equation (5), and omitting constraint correction.

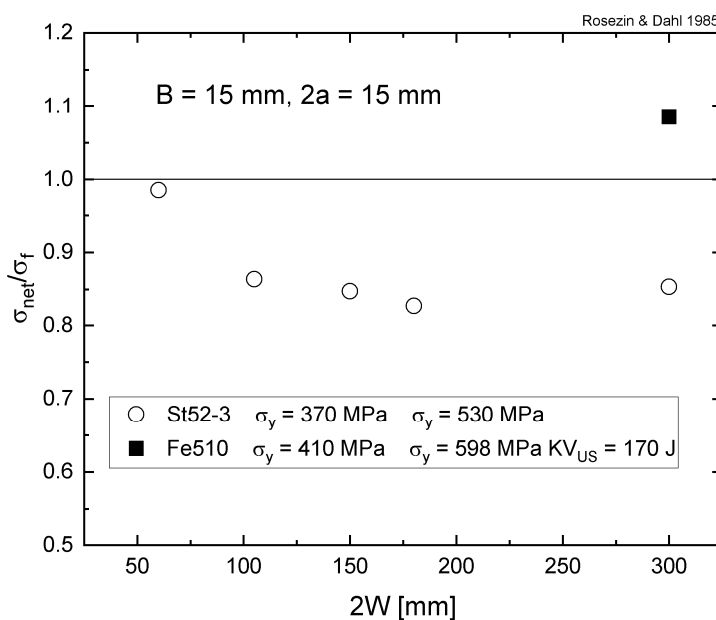


Figure 17. Proportional net section stress as a function of specimen width for 15 mm thick specimens with fixed flaw size, $2a = 15$ mm [11,12].

Overall, the present work provides an experimental validation of the criterion and methodology developed previously [1].

The original Charpy-V criterion for the limit load [1] assumes a high-constraint geometry. If the principle is applied to simple tension-loaded surface-cracked structures, the criterion can be relaxed. Figure 18 shows the Q-parameter values for shallow surface-cracked tension specimens [5,13,14]. Except for the crack ends, the stress-normalized Q is close to -0.5 . This enables a constraint correction to the criterion given in [1]. Following the same calculations as in [1] but correcting the crack driving force for constraint leads to a new criterion for the Charpy-V energy. The $J_{1\text{mm}}$ criterion was used because it proved to describe the CC(T) specimens well. The resulting criterion is shown in Figure 19.

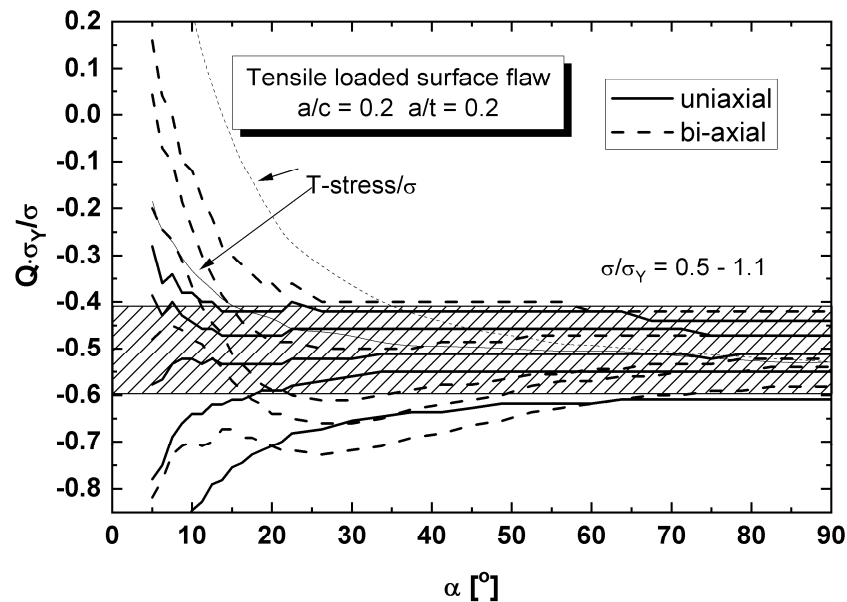


Figure 18. Comparison of angular dependence of elastic–plastic Q parameter normalized by relative stress and elastic T-stress for shallow uniaxial and biaxial tensile-loaded surface flaws [5,13,14].

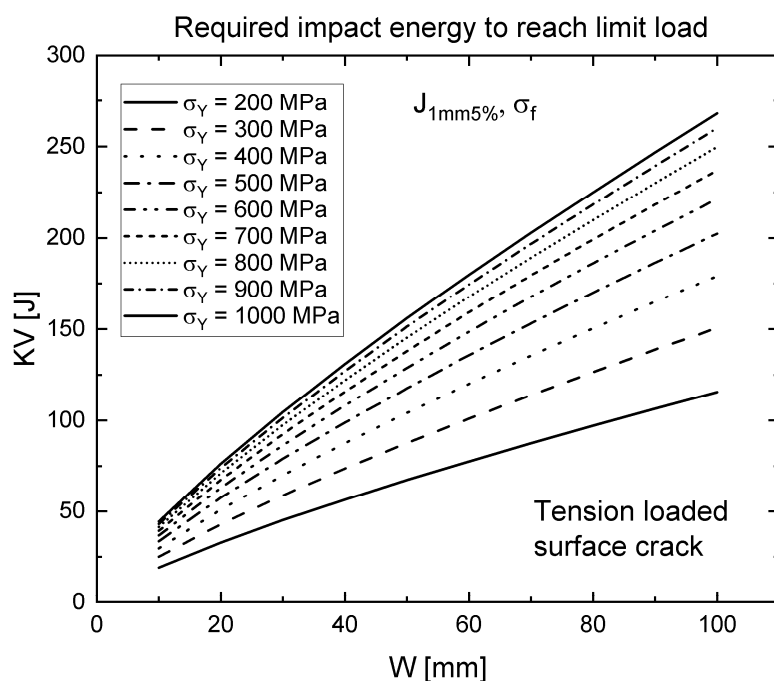


Figure 19. Charpy-V impact energy requirements to ensure plastic collapse for $J_{1\text{mm}}$, as a function of section thickness for tension-loaded surface flaws. The estimate is based on the 5% lower-bound Charpy-V correlation and accounting for the lower constraint.

The curves in Figure 19 can be approximated by Equation (15), which is a fit to the data in the figure.

$$KV(J_{1mm}) \geq \exp \left\{ 2.69 + 0.78 \cdot \ln(W) - \sqrt{\frac{480}{\sigma_y}} \right\} \quad (15)$$

The previous criterion [1] also has a requirement for temperature. Equation (16). This too can be adjusted for constraint, simply by adjusting the temperature by Equation (17) [5], where ΔT_{PC} corresponds to the temperature shift due to T-stress.

$$T_{PC} \geq T_{KV27J} - 536 + \frac{9742}{\sigma_Y} + 40.31 \cdot \ln(W) + 65.28 \cdot \ln(\sigma_Y) - \frac{71452}{W \cdot \sigma_Y} \quad (16)$$

$$\Delta T_{PC} = \frac{T_{stress}}{12 \text{ MPa}/^\circ\text{C}} \quad (17)$$

The temperature T_{PC} gives the lowest temperature where plastic collapse is predicted, provided that the Charpy-V impact energy at T_{PC} (or lower) fulfills Equation (15). The Charpy-V data do not need to correspond to the upper shelf, as the plastic collapse criterion does not intend to guarantee upper-shelf behavior of the structure. It only guarantees plastic collapse prior to any possible brittle fracture. If the low-constraint condition of the application cannot be guaranteed, the criterion in [1] should be used.

The above criteria regarding impact energy and temperature are valid for structures in quasistatic loading, even though based on a correlation between impact energy from a dynamic test. The correlation is only used to estimate the quasistatic tearing resistance of the material. Dynamic loading as in the case of an earthquake requires additional corrections both for impact energy and temperature.

It should be noted that the present criterion is aimed at low-constraint steel structures covered by Eurocode 3 and is not intended for pressure equipment, such as piping or pressure vessels, or steel structures where large thermal or residual stresses are present. It can only be used if residual stresses and constraints can be ruled out.

5. Conclusions

The load-bearing capacity of a CC(T) specimen in the ductile fracture regime is usually controlled by plastic collapse. If the material's tearing resistance is sufficiently low, the load-bearing capacity can drop below the plastic collapse value. Here, a recently developed simple fracture mechanics-based Charpy-V impact energy criterion for plastic collapse was used to provide a best estimate assessment of CC(T) specimen load-bearing capacity. The previous criterion was modified to specifically address the CC(T) specimen geometry with respect to crack driving force and limit load. In addition, the effect of the low constraint connected to the CC(T) specimen was accounted for with respect to ductile tearing. Because the goal was a best estimate, the mean J_{1mm} -CVNus correlation was used. It was shown that if the material's Charpy-V impact energy in relation to the material's yield strength is below a specific value, the load-bearing capacity will be less than the plastic limit load. This result verifies the previously developed simple fracture mechanics-based Charpy-V impact energy criterion for plastic collapse. A new criterion, specifically for tension-loaded surface flaws, was developed, in line with the previous high-constraint criterion. The present criterion is limited to steel structures covered by Eurocode 3. It is not intended for pressure equipment such as piping or pressure vessels, or steel structures where large thermal or residual stresses are present. It cannot be used if residual stresses and constraints may be present in the structure. If the low-constraint condition of the application cannot be guaranteed, the high-constraint criterion should be used.

Funding: This research received no external funding.

Institutional Review Board Statement: Not applicable.

Informed Consent Statement: Not applicable.

Data Availability Statement: Not applicable.

Conflicts of Interest: The author declares no conflict of interest.

References

1. Wallin, K. A simple fracture mechanics based Charpy-V impact energy criterion for plastic collapse. *Eng. Fract. Mech.* **2020**, *237*, e107247. [[CrossRef](#)]
2. Tada, H.; Paris, P.C.; Irwin, G.R. *The Stress Analysis of Cracks Handbook*, 2nd ed.; Paris Productions Incorporated: St. Louis, MO, USA, 1985.
3. Miller, A.G. Review of limit loads of structures containing defects. *Int. J. PVP* **1988**, *32*, 197–327. [[CrossRef](#)]
4. Wallin, K. Low-cost J-R curve estimation based on CVN upper shelf energy. *Fatigue Fract. Eng. Mater. Struct.* **2001**, *24*, 537–549. [[CrossRef](#)]
5. Wallin, K. *Fracture Toughness of Engineering Materials—Estimation and Application*; EMAS Publishing: Warrington, UK, 2011.
6. O'Dowd, N.P.; Shih, C.F. Family of Crack-Tip Fields Characterized by a Triaxiality Parameter. II. Fracture applications. *J. Mech. Phys. Solids* **1992**, *40*, 939–963. [[CrossRef](#)]
7. Brocks, W.; Schmitt, W. *Quantitative Assessment of the Role of Crack Tip Constraint on Ductile Tearing*; ASTM International: West Conshohocken, PA, USA, 1993; pp. 64–78.
8. Feldmann, M.; Schaffrath, S.; Citarelli, S. *Approach for Upper-Shelf Toughness Requirements for the Design of Steel Structures Based on Damage Mechanics*; CEN/TC 250/SC 3 N 3162; RWTH Aachen University: Aachen, Germany, July 2020.
9. Dahl, W.; Hesse, W. Auswirkung der Beurteilung von Stählen auf die Anwendung im Hoch- und Anlagenbau. *Stahl Eisen* **1986**, *106*, 695–702.
10. Hubo, R.; Twickler, W.; Hesse, W.; Dahl, W. Failure behaviour of steels with different levels of strength and toughness. *Nucl. Eng. Des.* **1988**, *108*, 457–466. [[CrossRef](#)]
11. Rosezin, H.-J.; Dahl, W. Einfluss von Temperatur und Probengeometrie auf die Ergebnisse von Grosszugversuchen. *Stahl Eisen* **1985**, *105*, 523–529.
12. Dormagen, D.; Halim, A.; Ehrhardt, H.; Dahl, W. On the toughness evaluation of sulphide-controlled Fe510 steel by Charpy-V-impact, fracture mechanics and wide plate tests. In *The Crack Tip Opening Displacement in Elastic-Plastic Fracture Mechanics*; Schwalbe, K.H., Ed.; Springer: Berlin/Heidelberg, Germany, 1986. [[CrossRef](#)]
13. Wang, X. Two-Parameter Characterization of Elastic-Plastic crack Front Fields: Surface Cracked Plates under Tensile Loading. *Eng. Fract. Mech.* **2009**, *76*, 958–982. [[CrossRef](#)]
14. Wang, X. Elastic T-stress Solutions for Semi-Elliptical Surface Cracks in Finite Thickness Plates. *Eng. Fract. Mech.* **2003**, *70*, 731–756. [[CrossRef](#)]